#### **NURETH14-451**

# COMPUTATIONAL STUDY OF FLOW AND HEAT TRANSFER FOR WATER UNDER SUPERCRITICAL CONDITIONS IN A VERTICAL PIPE USING NAFA CFD CODE

## A. M. Vaidya, N. K. Maheshwari, P. K. Vijayan and D. Saha

Reactor Engineering Division, Bhabha Atomic Research Centre, Mumbai, India

#### Abstract

The objective of this work is to study the flow and heat transfer for water under super-critical conditions. Two dimensional (axi-symmetric) CFD simulation is performed for this purpose using an in-house developed code named NAFA. The flow is computed for vertically upward as well as downward orientations. Further, for each orientation, wide range of heat flux is considered. It is found that for downward flow, heat transfer coefficient is higher than that for upward flow, other conditions remaining same. The heat transfer characteristics are found to be dependent on the pipe outlet temperature with reference to pseudo-critical temperature.

#### 1. Introduction

The objective of this work is to perform computational analysis of heat transfer and fluid flow in a super-critical water flowing in vertical tube. It is established fact that the heat transfer characteristics of a flow at super-critical conditions are much different than those at sub-critical conditions. This is due to the fact that the thermo-physical properties at super-critical conditions are much different than those at sub-critical conditions [1]. The heat transfer at super-critical conditions depends on various aspects like geometry, length and diameter of pipe, orientation of flow with respect to gravity, operating pressure, heat flux, mass flux, working fluid, etc. For design of Super-Critical Water Reactors (SCWRs), it is important to have a thorough understanding of the heat transfer characteristics.

## 2. Survey of previous research on heat transfer in super-critical flows

The subject of super-critical heat transfer is being studied using experimental techniques since last 50 years. More recently, in last 10 years, numerical simulation of super-critical flow using system codes as well as CFD codes is being performed. In these studies, the heat transfer characteristics are studied for super-critical water as well as CO<sub>2</sub>. Yamagata et al. [2] performed experimental investigation with water as working fluid. The data was generated for different heat fluxes, mass fluxes and operating pressures in vertical and horizontal pipes. He found that, for a given mass flux and heat flux, the heat transfer coefficient shows a peak at pseudo critical temperature at a given pressure. Also, with increase in heat flux, the peak of heat transfer reduces eventually resulting in deteriorated heat transfer. They proposed a correlation for heat transfer coefficient under enhanced heat transfer regime for water. Also a correlation for determining onset of heat transfer deterioration for water has been proposed. The experiments of Yamagata et al were at relatively high mass flux conditions (1260 kg/m²-s). Shitsman performed experiments under low mass flux conditions (430 kg/m²-s) by varying heat flux for this mass flux. Shitsman

also found that with increase in heat flux beyond a certain value, heat transfer deterioration occurs. Miropol'skii and Shitsman also proposed a correlation for predicting the heat transfer coefficient [1]. It should be noted that, though deterioration is found for high mass flux as well as low mass flux conditions, the physical mechanism by which deterioration occurs differs for the two conditions. At low mass flux conditions, the laminarization at near wall due to large buoyancy forces results in reduced turbulent heat transfer in radial direction. In high mass flux cases, the increase in laminar sub-layer thickness results in deterioration. Bae et al. [3] performed experimental investigation of heat transfer for CO<sub>2</sub> flowing upwards and downwards in vertical tube for various heat and mass flux fluxes and operating pressures. Pioro et al. [1] performed survey of various empirical correlations and compared their predictions with experimental data of Shitsman and that obtained at Chalk River Lab (AECL, Canada). They found that, none of the correlations were able to qualitatively and quantitatively able to reproduce the experimental data. Further, they mentioned that these correlations do not apply to deteriorated heat transfer regime. Yang et al. [4] and Cheng et al. [5] performed numerical simulation of super-critical water flow in pipe as well as fuel rod bundles. The flow through pipe is simulated using various turbulence models. Yang et al. [4] simulated experiments of Yamagata et al. They found that the low Reynolds number models were not able to accurately predict the wall temperature data (at heat flux 698 kW/m<sup>2</sup>). They found that, all other turbulence models including high Reynolds number versions of k-ε model and two layer turbulence models give almost same predictions. It should be noted that this conclusion is based on simulation of enhanced heat transfer regime only. Cheng et al. [5] simulated experiments of Yamagata et al. They used ANSYS CFD for this purpose. They applied standard k-\varepsilon model, RNG k-\varepsilon model and 2<sup>nd</sup> order closure models also. They found that except RNG k-ε model, all other models were able to reasonably simulate the test data. The ωtype models were also tested. They found that ω-type models completely failed to match the test data in the pseudo-critical region. Seo et al. [6] studied the applicability of RANS (Reynolds Averaged Navier-Stokes equations) based approach for various regimes of super-critical heat transfer. They explained that during Reynolds averaging, in variable property situation, many terms cannot be modeled and are neglected. Due to this limitation in the mathematical treatment, RANS approach will have limitations in certain regimes. The authors performed analysis and estimated the regimes of heat transfer in which RANS will fail to predict. Ambrosini [13] numerically studied the supercritical heat transfer phenomenon in the deterioration regime. He applied a number of low Reynolds number versions of k-E model for the simulation. He found that qualitatively all models give similar result with experimental data. However, none of the models predicted the extent of deterioration in agreement with experimental data. Only Yang and Shih version of low Re turbulence model could predict the onset of deterioration in agreement with experimental data.

#### 3. Present work

In this work, computational analysis is performed. The effect of (i) flow orientation with respect to gravity and (ii) heat flux is studied. The study is performed using NAFA CFD code. NAFA is an acronym for Numerical Analysis of Flows in Axi-symmetric geometries. The mathematical details of the code, its validation and some applications to super-critical heat transfer are published elsewhere by the authors [7, 8] and some important details will be given later in this paper.

The objective of the work is to study two important parameters (direction with respect to gravity and heat flux) affecting the heat transfer characteristics. The flow in vertically upward and downward conditions is studied. Also, for each orientation, wide range of heat flux is considered. This is done to vary the relative influence of inertia and buoyancy forces.

## 4. Computational methodology

Before discussing the case studies, few important details of NAFA code used for this work are given in this section. NAFA can handle laminar/ turbulent flows under sub-critical/super-critical flow conditions with/without heat transfer. It can handle pipe and annulus geometries. Conservation equations of mass, momentum, energy, turbulent kinetic energy and its rate of dissipation are solved numerically using Finite Volume technique [9]. The pressure-velocity coupling is performed as per SIMPLE algorithm [9]. For modeling turbulence, at present, the high Reynolds number standard k-ɛ model with standard wall functions is implemented [10, 11]. Variable property formulation is used. The code incorporates four boundary conditions namely "VELOCITY INLET", "WALL", "AXIS" and "OUTLET" as shown in Figure 1. In the code, convection terms of all equations except energy equation are modeled as power law scheme [9] and the convection terms of energy equation is modeled as per 2<sup>nd</sup> order upwind scheme for more accuracy.

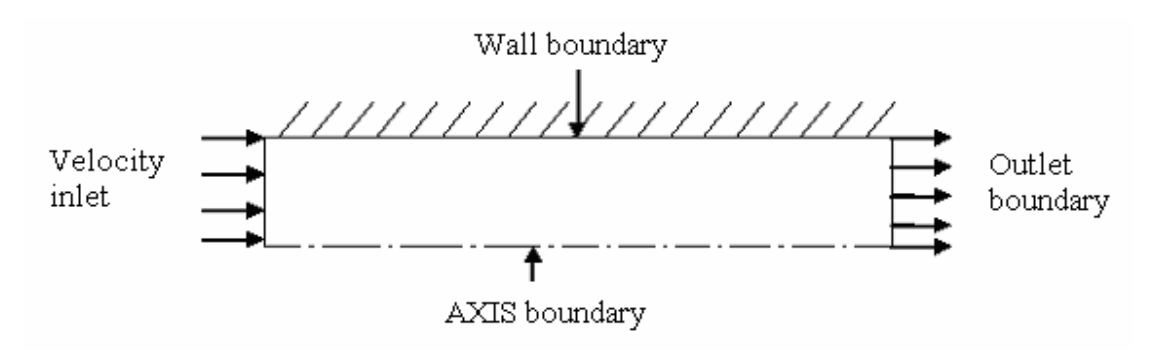


Figure 1 Computational domain and boundary conditions for pipe flow

#### 4.1 Choice of turbulence model

Previously, various authors have performed simulation with varied turbulence models. These authors have used commercial softwares wherein different models are readily available. The authors have developed their own code indigenously. As a first step, standard k- $\epsilon$  turbulence model has been implemented. Nonetheless, as is evident from the literary survey given above, different researchers have different opinions regarding suitable selection of turbulence model for supercritical application. Hence it was decided to generate result with a high Reynolds number turbulence model first. The scope of this paper is limited to the presentation of results of standard k- $\epsilon$  turbulence model with standard wall functions. As a next step, the low Reynolds number variant of k- $\epsilon$  model is being implemented in NAFA. However it should be noted that, as noted by Seo et al. [6], during Reynolds averaging, certain terms are dropped and hence even the most elaborate turbulence model won't be able to exactly reproduce the experimental results in all conditions.

#### 4.2 Thermo-physical properties

The fluid properties (i.e. viscosity, conductivity, density and specific heat) required for solving these equations are strongly dependent on temperature at super-critical pressure. NAFA has provision to read properties in tabular form. Piecewise linear interpolation is used. The isobaric properties are taken from NIST online property calculator [12]. At a given pressure, typically 200 points map the data with temperature step of 1°C. It is found that, if the same data is also represented by 30 points, with peak of specific heat captured properly and with more points in the large gradient region, then also the results are not affected. (These results are not reported here for brevity). The properties provided by NIST calculator are taken to be accurate enough for present work. The analysis of effect of uncertainties in property calculation on final computational results is beyond the scope of this paper/work. These properties are used by many authors previously.

#### 4.3 Validation

NAFA is validated by applying to Yamagata's test cases. Experimental investigation of turbulent super-critical flows in horizontal and vertical pipes has been done by Yamagata et al. [2]. They have presented experimental data for flow of water through pipe at 245 bar. Mass flux is maintained constant at 1260 kg/m²-s. Wall temperature data for different heat fluxes ranging from 233 kW/m² to 930 kW/m² is reported. This wall temperature data is used for validation. The comparison of the NAFA results with Yamagata's data is shown in Figure 2. It can be seen that the agreement between computational results and experimental data, upto heat flux of 698 kW/m² is acceptable, beyond which there is some deviation. Thus, it can be seen that, except for very high heat flux, the CFD code is able to predict wall temperatures reasonably well. The experimental data chosen is for upward flow of water.

## 4.4 Simulation inputs

The results are generated for flow of water in vertical pipe in upward and downward orientations. The operating and design conditions are summarised in following table. These conditions are typical of a SCWR.

The flow is influenced by (i) operating pressure, (ii) mass flux at inlet, (iii) surface heat flux, (iv) length of pipe (affects the hydrostatic head and buoyancy), (v) pipe diameter, (vi) working fluid, (vii) inlet temperature and (viii) direction (with respect to gravity). In the present study, effect of heat flux and heat fluxes is studied. Flow is modelled as incompressible because the pressure variation from inlet to outlet is negligible compared to operating pressure. The properties of water are assumed to be dependent only on temperature. The properties are shown in

Figure 3 and Figure 4 [12].

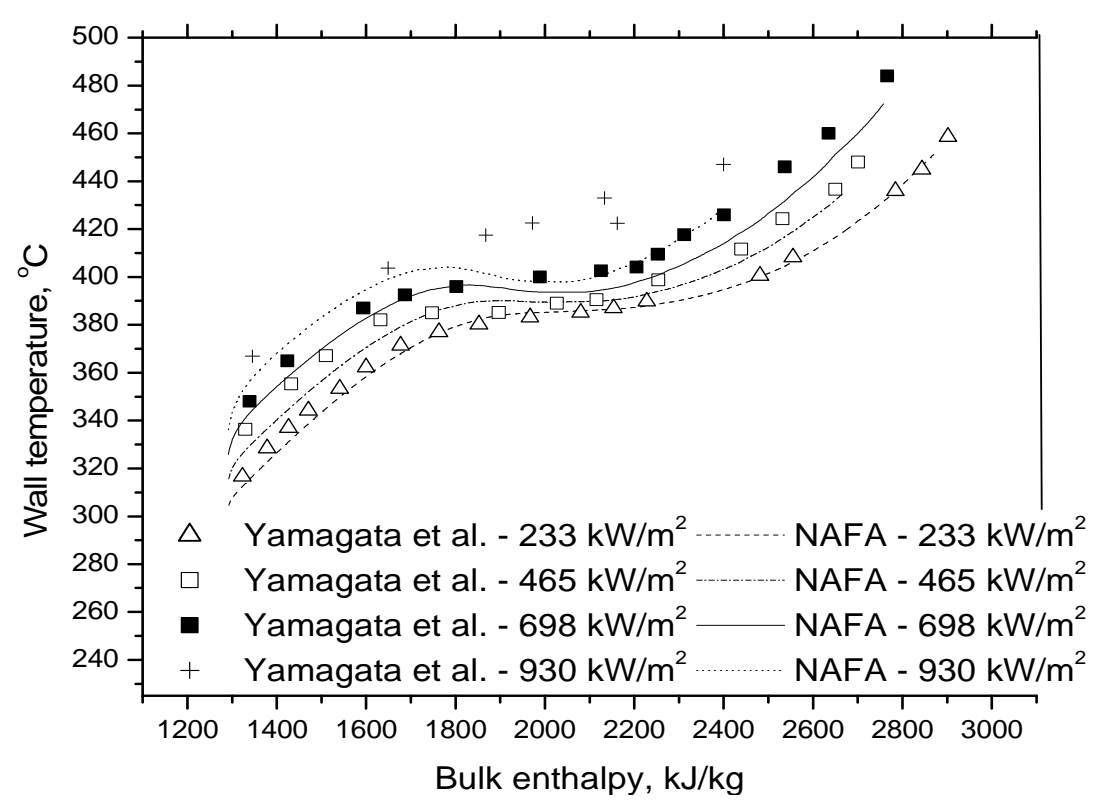


Figure 2 Comparison of computational result with experiment data (for wall temperature vs. bulk enthalpy at different heat fluxes)

Inner Dia. of pipe	8 mm
Length	3.3 m
Working fluid	Water
Pressure	250 bar
Heat flux	$100 - 400 \text{ kW/m}^2$
Mass flux	$315 \text{ kg/m}^2\text{-s}$
T <sub>inlet</sub>	100°C & 350°C
Flow direction	Upward and downward

Table 1 Operating and design conditions

## 4.5 Grid independence study

The first step is to establish the minimum grid requirement for generating grid independent results. For this, the number of cells in axial direction was fixed at 350 and the number of cells in radial direction is changed. The results for 15 and 30 number of cells in radial direction are obtained and compared. Figure 5 shows the variation of heat transfer coefficient with bulk

temperature. It is seen that both the grids generate the same result. Fixing number of cells in radial direction at 30, the number of cells in axial direction is changed from 350 to 700. The axial variation of centerline temperature for the two grids is shown in Figure 6. It can be seen that both the grids give same result. Thus, the grid independence study shows that the results are not dependent on grid for a grid of  $15 \times 350$  and higher.

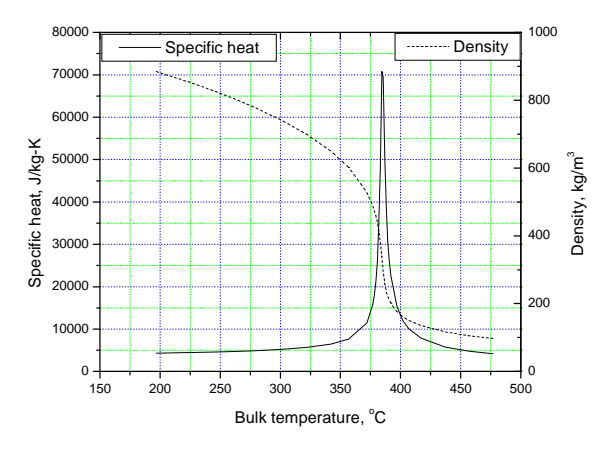


Figure 3 Variation of specific heat and density with temperature at 250 bar

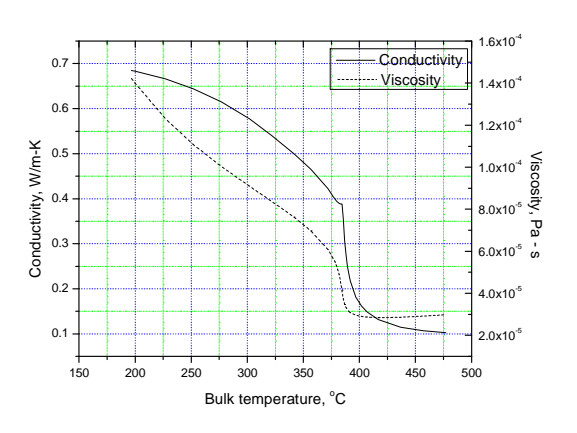


Figure 4 Variation of conductivity and viscosity with temperature at 250 bar

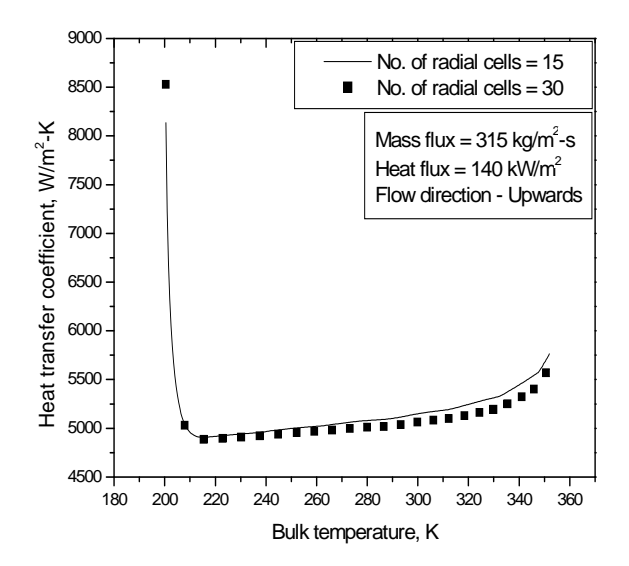


Figure 5 Variation of heat transfer coefficient computed by two different grids

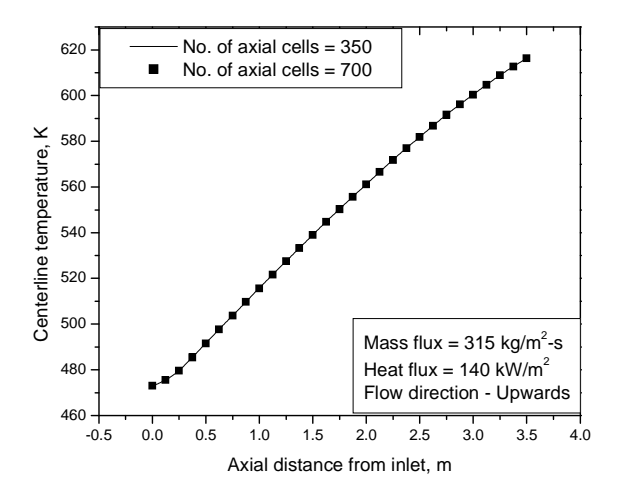


Figure 6 Variation of centerline temperature computed by two different grids

## 5. Results and Discussion

The results for upward and downward flows are generated. In these simulations, mass flux is fixed at 315 kg/m<sup>2</sup>-s. Length is fixed at 3.3 m out of which first 0.5 m is unheated. The unheated

part helps to achieve a fully developed velocity profile at inlet to heated section. Operating pressure is fixed at 250 bar. Keeping mass flux, length and operating pressure constant, various results are generated by varying inlet temperature and heat flux.

For systematic study of the heat transfer characteristics of upward and downward flows, two sets of results are generated. In both the sets, inlet temperature is taken to be less than the pseudo-critical temperature (which is 385°C at 250 bar). But in 1<sup>st</sup> set, outlet temperature is less than pseudo-critical temperature and in 2<sup>nd</sup> set, the outlet temperature is more than pseudo-critical temperature. This is done by adjusting the inlet temperature and heat flux.

In first set, inlet temperature is fixed at  $100^{\circ}$ C. The heat flux is varied from  $100 \text{ kW/m}^2$  to  $300 \text{ kW/m}^2$ . This makes it sure that the outlet temperature is less than pseudo-critical temperature even for highest heat flux of  $300 \text{ kW/m}^2$ . Both upflow and downflow conditions are simulated.

In  $2^{nd}$  set, inlet temperature is fixed at  $350^{\circ}$ C. The heat flux is varied from  $100 \text{ kW/m}^2$  to  $500 \text{ kW/m}^2$ . This makes it sure that the outlet temperature is more than pseudo-critical temperature even for smallest heat flux of  $100 \text{ kW/m}^2$ .

## 5.1 Results of 1<sup>st</sup> set

Figure 7 shows the variation of heat transfer coefficient with bulk temperature for heat flux of 100 kW/m². Calculation of heat transfer coefficient is explained in Appendix – A. It is observed that the HTC of downflow is more than upflow throughout the range of bulk temperature considered. Figure 8 shows the variation of heat transfer coefficient with bulk temperature for heat flux of 200 kW/m². Again, the heat transfer coefficient is more in downflow. It is seen that with bulk temperature approaching pseudo-critical value, the difference in downflow and upflow heat transfer coefficient increases. Figure 9 shows the variation of heat transfer coefficient with bulk temperature for heat flux of 300 kW/m². Here, it is seen that in downflow, the heat transfer coefficient monotonically increases over entire range of bulk temperature (excepting the entrance region). But in upflow, the heat transfer coefficient increases upto 175°C. From 175°C to 225°C, it reduces. From 225°C to 325°C, it rises gradually. Beyond 325°C, it rises rapidly.

## 5.1.1 <u>Discussion</u>

From inlet to outlet, the bulk temperature increases (due to uniform surface heat flux). As seen from property variation, density continuously decreases with increase in temperature. Thus, density continuously decreases from inlet to outlet. Due to reducing density, flow tends to accelerate.

In downward flow, gravity is in same direction as acceleration. Lighter fluid is at lower elevation and heavier fluid is at higher elevation. Hence the buoyancy force is in opposite direction of the gravity and acceleration. It is seen that the gravity and acceleration is much more predominant than upward buoyancy. Hence heat transfer coefficient increases continuously. This is observed at all the heat fluxes.

In upward flow, the lighter fluid is at top and heavier fluid is at bottom. The buoyancy force and fluid acceleration are in same direction but gravity is in opposite direction. Upto 350°C, there is gradual reduction in density causing some flow acceleration and upward buoyancy force but

gravity force is in opposite direction. Due to this, the heat transfer coefficient at a given bulk temperature is less than downward flow. Beyond 350°C, there is rapid decrease in density causing rapid acceleration and large buoyancy effect. This overcomes the opposing gravity and hence the heat transfer coefficient in upward flow almost reaches the downflow value.

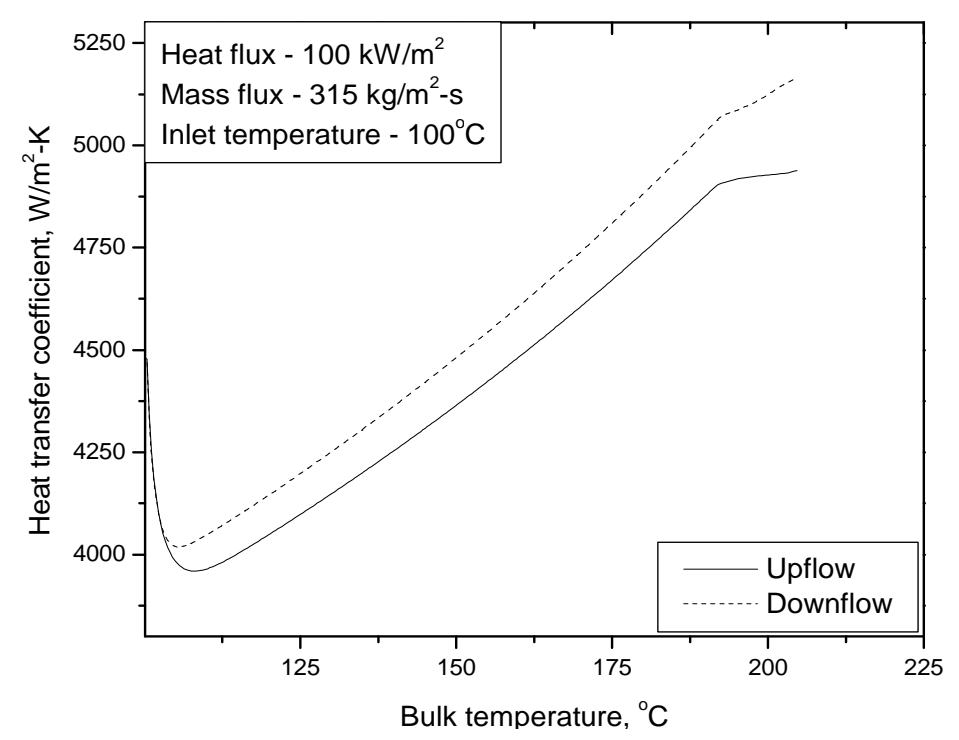


Figure 7 Variation of heat transfer coefficient with bulk temperature for heat flux of 100 kW/m<sup>2</sup>

## 5.1.2 Effect of heat flux on heat transfer coefficient for 1<sup>st</sup> set

Figure 10 shows the effect of heat flux on heat transfer coefficient for upflow case. Prediction of Dittus-Boelter correlation<sup>1</sup> is plotted for reference. With increase in heat flux beyond 200 kW/m<sup>2</sup>, the supercritical heat transfer coefficient is less than that predicted by Dittus-Boelter correlation indicating deterioration in heat transfer. Yamagata's correlation for heat transfer deterioration is given by following expression.

$$q'' = 0.2G^{1.2} \tag{1}$$

where q" is heat flux in  $kW/m^2$  and G is mass flux in  $kg/m^2$ -s. As per Eq.(1), for mass flux of 315  $kg/m^2$ -s, heat transfer deterioration should occur at and beyond heat flux of 199  $kW/m^2$ . The present findings are consistent with Yamagata's correlation.

Figure 11 shows the effect of heat flux on heat transfer coefficient for downflow case. In this case, at all heat fluxes, heat transfer enhancement is observed. With increase in heat flux, there is slight increase in heat transfer coefficient. Thus for downflow, increase in heat flux does not immediately result into heat transfer deterioration.

<sup>&</sup>lt;sup>1</sup> Dittus-Boelter correlation -  $Nu = 0.023 \,\mathrm{Re}^{0.8} \,\mathrm{Pr}^{0.4}$  (all properties evaluated at bulk temperature)

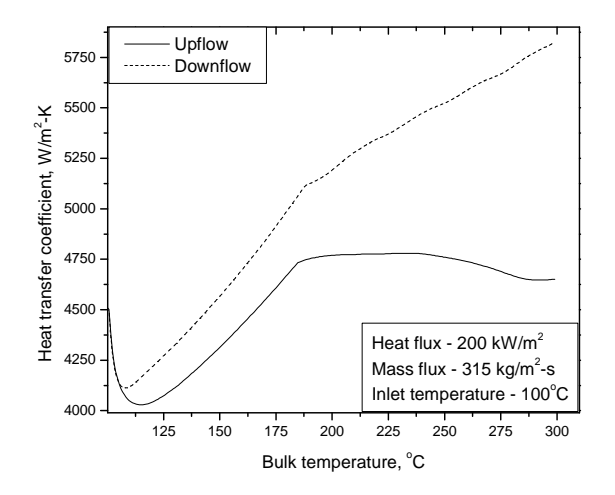


Figure 8 Variation of heat transfer coefficient with bulk temperature for heat flux of 200  $kW/m^2$ 

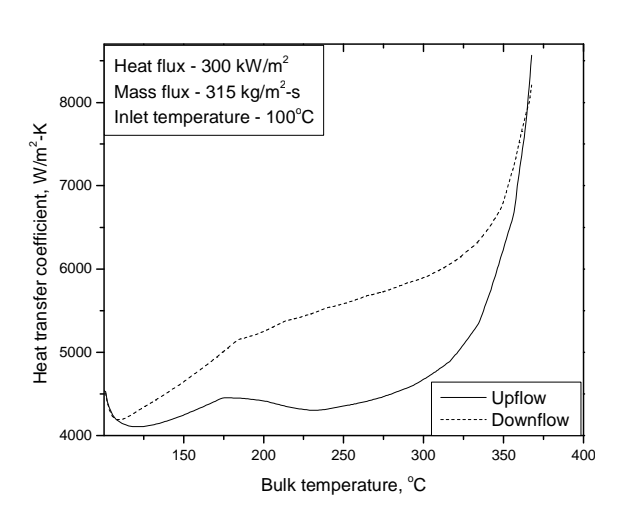


Figure 9 Variation of heat transfer coefficient with bulk temperature for heat flux of 300 kW/m<sup>2</sup>

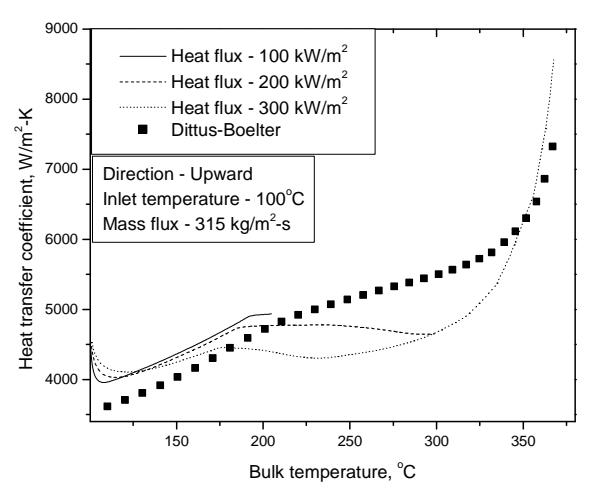


Figure 10 Effect of heat flux on heat transfer coefficient for upflow

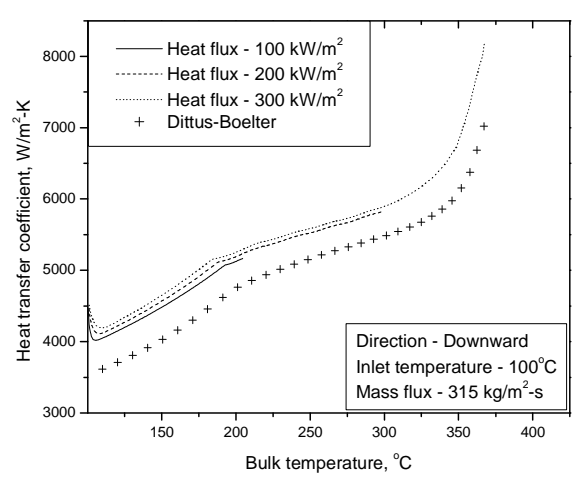


Figure 11 Effect of heat flux on heat transfer coefficient for downflow

## 5.2 Results of 2<sup>nd</sup> set

Figure 12 shows the Variation of heat transfer coefficient with bulk temperature for heat flux of 200 kW/m² for this case (in which inlet temperature is increased to 350°C, compared to 100°C of previous set). Figure 13 and Figure 14 show the same result for heat flux of 300 kW/m² and 400 kW/m². It can be seen that with increase in heat flux, in region before pseudo-critical temperature, the heat transfer coefficient of upflow is higher than that in downflow. In region beyond pseudo-critical temperature, the heat transfer coefficient of downflow is consistently higher than upflow.

# 5.2.1 Effect of heat flux on heat transfer coefficient for 2<sup>nd</sup> set

Figure 15 shows the effect of heat flux on heat transfer coefficient for upflow case (length, mass flux, operating pressure kept constant). Figure 16 shows the same result for downflow. The prediction of Dittus-Boelter correlation is given for reference. In both cases, before pseudocritical temperature, there is gradual increase in heat transfer coefficient with increase in heat flux. Beyond pseudo-critical temperature, for both the cases, there is gradual decrease in heat transfer coefficient with increase in heat flux. Comparing with Dittus-Boelter correlation, in upflow as well as downflow, before pseudo-critical temperature, slight heat transfer enhancement is observed. Beyond pseudo-critical point, for upflow as well as downflow, there is only slight reduction in heat transfer but deterioration is not observed.

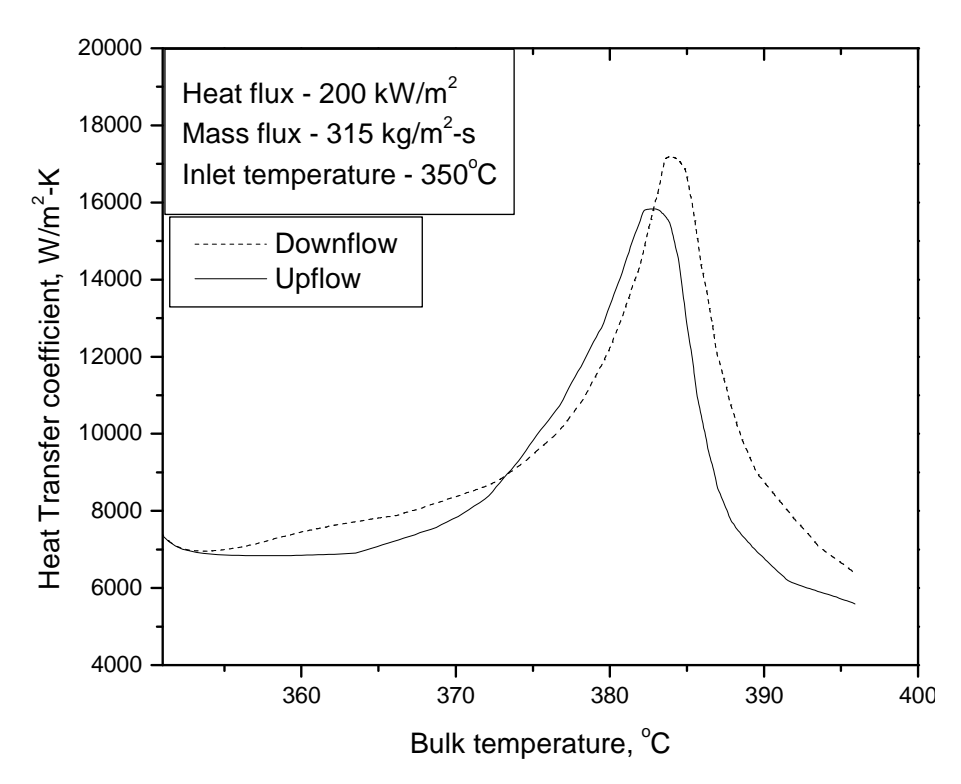


Figure 12 Variation of heat transfer coefficient with bulk temperature for heat flux of 200 kW/m<sup>2</sup>

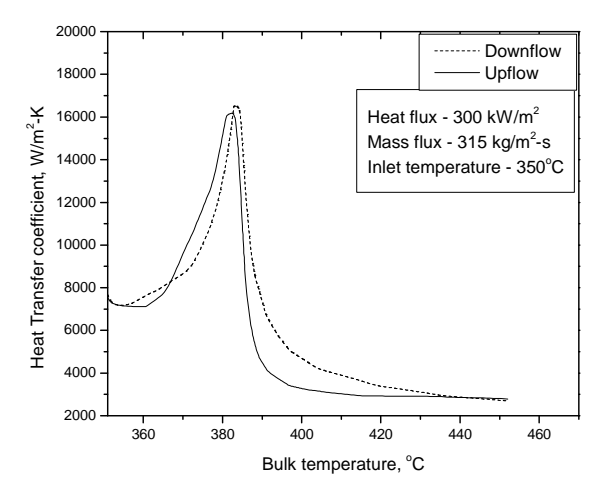


Figure 13 Variation of heat transfer coefficient with bulk temperature for heat flux of 300  $kW/m^2$ 

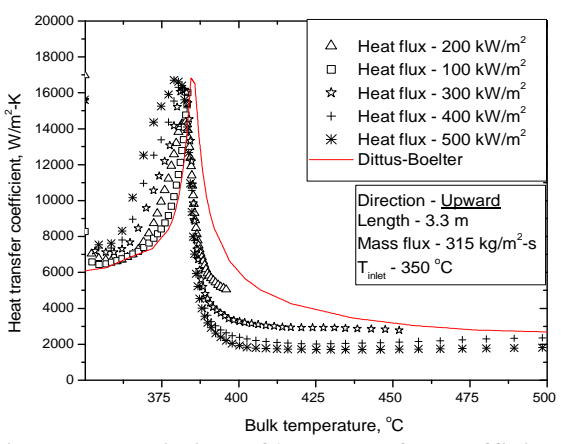


Figure 15 Variation of heat transfer coefficient with bulk temperature for various heat fluxes for upflow

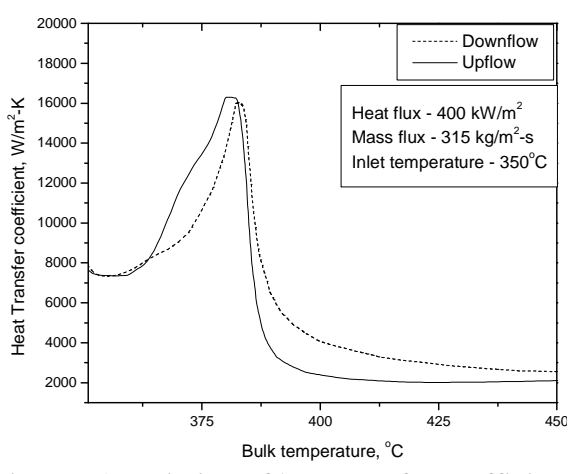


Figure 14 Variation of heat transfer coefficient with bulk temperature for heat flux of 400  $kW/m^2$ 

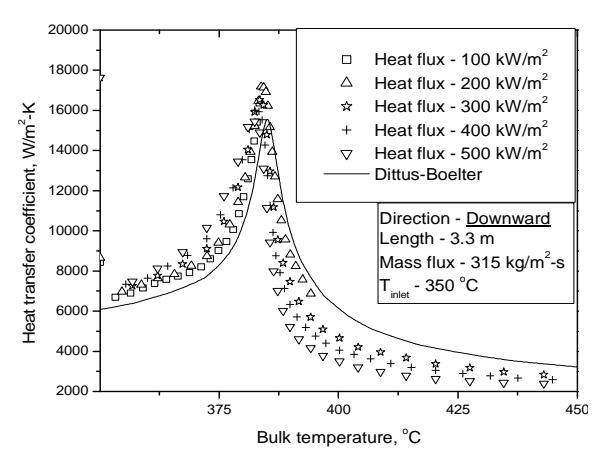


Figure 16 Variation of heat transfer coefficient with bulk temperature for various heat fluxes for downflow

#### 5.3 Discussion

It should be noted that, in validation exercise, in the cases where q/G > 0.55, deviation of computational results from experimental data is obtained. In this section, results are given upto q/G = 1.5. The authors plan to regenerate these results with a modified code in which a different turbulence model will be incorporated.

#### 6. Conclusions

Computational study of super-critical flow of water in vertical pipe for upward and downward directions is performed. The study is performed using an indigenously developed and validated code named NAFA. The effect of heat flux on upward and downward flows is studied using the code.

Two sets of results are generated. In 1<sup>st</sup> set where pipe outlet temperature is less than pseudo-critical temperature, it is found that the downflow gives consistently higher heat transfer coefficient than upflow over the considered range of heat fluxes. With increase in heat flux, for upflow, heat transfer deterioration is observed. Computational estimated deterioration heat flux matches well with Yamagata's correlation for upflow. For downflow, the heat transfer deterioration is not observed.

In 2<sup>nd</sup> set where pipe outlet temperature is beyond pseudo-critical temperature, heat transfer characteristics are somewhat different. In this case, for upflow as well as downflow, before pseudo-critical point, heat transfer slightly increases with heat flux. Beyond pseudo-critical point, in upflow and downflow, heat transfer slightly reduces but deterioration is not observed.

Thus, the heat transfer characteristics of supercritical pipe flow are found to be affected by flow direction as well as the value of outlet temperature with respect to pseudo-critical temperature.

#### References

- [1] I. L. Pioro, F. K. Hussam, R. B. Duffey, "Heat transfer to super-critical fluids flowing in channels empirical correlations (survey)", *Nuclear Engineering and Design*, Vol. 230, 2004, pp. 69-91.
- [2] K. Yamagata, K. Nishikawa, S. Hasegawa, T. Fujii, S. Yoshida, "Forced convective heat transfer to super-critical water flowing in tubes", *Int. J. Heat and Mass Transfer*, Vol. 15, 1972, p.p. 2575 2593.
- [3] Y.-Y. Bae, H.-Y. Kim, D.-J. Kang, "Forced and mixed convection heat transfer to supercritical CO<sub>2</sub> vertically flowing in a uniformly-heated circular tube", *Experimental Thermal and Fluid Science* Vol. 34, 2010, pp. 1295–1308
- [4] Y. Jue, Y. Oka, Y. Ishiwatari, J. Liu and J. Yoo, "Numerical investigation of heat transfer in upward flows of super-critical water in circular tubes and tight fuel rod bundles", *NED*, Vol. 237, 2007, pp. 420-430.
- [5] X. Cheng, B. Kuang and Y. H. Yang, "Numerical analysis of heat transfer in super-critical water cooled flow channels", *NED*, Vol. 237, 2007, pp. 240-252.
- [6] K. W. Seo, M. H. Kim, M. H. Anderson, M. L. Corradini, "Heat transfer in a supercritical fluid: Classification of heat transfer regimes", *Nuclear Sci & Technology*, Vol. 154, June, 2006.
- [7] A. M. Vaidya, N. K. Maheshwari, P. K. Vijayan and D. Saha, "Development, validation and application of NAFA 2D-CFD code", BARC Report, BARC/2010/E/001, Mumbai, 2010.
- [8] A. M. Vaidya, N. K. Maheshwari and P. K. Vijayan, "Development of NAFA code for computation of super-critical Flows", <u>Proc. Conf. Nuclear Reactor Technology-4</u>, BARC, India, March 4-6, 2011.

- [9] S. Patankar, "Numerical Heat Transfer and Fluid Flow", Taylor and Francis, 1980.
- [10] B. E. Launder and D. B. Spalding, "The numerical computation of turbulent flows", Computational Methods in Applied Mechanics and Engineering, Vol. 3, 1974, pp. 269 – 289
- [11] Biswas G. and Eswaran V., "Turbulent Flows: Fundamentals and Modelling", Narosa Publishing House, New Delhi 2000.
- [12] http://webbook.nist.gov/chemistry/fluid/
- [13] Ambrosini W., Lesson learned from the adoption of numerical techniques in the analysis of nuclear reactor thermal-hydraulic phenomena, Progress in Nuclear Energy, Vol. 50, 2008, pp 866–876

## Appendix - A

Procedure for calculating heat transfer coefficient

- (1) Based on inlet temperature, inlet enthalpy is computed from property tables.
- (2) Local bulk enthalpy at any location is computed from inlet enthalpy and heat addition from surface using following equation.

$$h_{b,x} = h_{in} + \frac{q''\pi \cdot d \cdot x}{m}$$

- (3) Corresponding local bulk temperature,  $T_{b,x}$  is computed from property tables.
- (4) Wall temperature at a given axial location is obtained from CFD code.
- (5) Heat transfer coefficient at given axial location is found out from following equation.

$$h = \frac{q''}{\left(T_{w,x} - T_{b,x}\right)}$$

(6) Alternately, instead of using  $T_{b,x}$  computed in above manner, at a given axial location, using the radial profile of temperature computed by CFD code, mass flow weighted mean temperature at the given axial location is computed. This in conjunction with wall temperature at that axial location can be used for computation of heat transfer coefficient. However, authors found that the two approaches give same numerical value of heat transfer coefficient (within < 1%).